



## Original Research Article

# Synthesis, Characterization, and Methyl Green Removal of Epichlorohydrin Crosslinked Schiff Base Chitosan/Fe<sub>2</sub>O<sub>3</sub> Nanocomposite

Arefeh Khalili<sup>1</sup>, Aliakbar Dehno Khalaji<sup>1,\*</sup>, Ali Mokhtari<sup>1</sup>, Mohsen Keyvanfard<sup>2</sup>

<sup>1</sup>Department of Chemistry, Faculty of Science, Golestan University, Gorgan, Iran

<sup>2</sup>Department of Chemistry, Faculty of Science, Islamic Azad University, Majlesi Branch, Iran

## ARTICLE INFO

## Article history

Submitted: 2021-06-15

Revised: 2021-09-05

Accepted: 2021-09-20

Available online: 2021-12-12

Manuscript ID: [PCBR-2106-1192](#)

DOI: [10.22034/pcbr.2021.290770.1192](https://doi.org/10.22034/pcbr.2021.290770.1192)

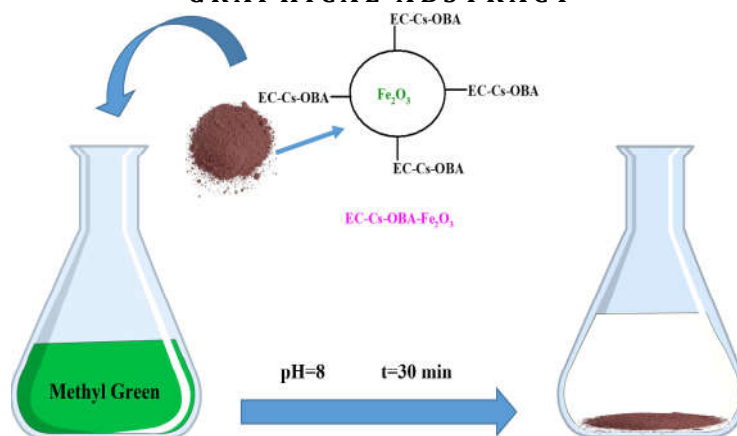
## KEYWORDS

Epichlorohydrin  
Crosslinked  
Schiff base chitosan  
Fe<sub>2</sub>O<sub>3</sub>  
Nanocomposite  
Methyl green removal

## ABSTRACT

Adsorption process has been widely used as one of the efficient methods in removing pollutants that are hardly biodegradable. In this study, new epichlorohydrine crosslinked Schiff base chitosan/Fe<sub>2</sub>O<sub>3</sub> nanocomposite was prepared and applied as adsorbent material. The synthesized adsorbent was characterized by FT-IR, XRD, TGA/DTA, DSC, EDS, BET, XRD and FE-SEM to explore morphology, structure and functional groups. The adsorbent was applied for removal of methyl green (MG) from aqueous solutions through batch experiments. Different parameters such as adsorbent dosage, pH and contact time were considered. The removal efficiency of 94.8 % was acquired at the optimum condition of pH = 8, adsorbent dosage of 0.02 g and contact time of 30 min. The adsorption capacity of the sorbent was found to be 47.4 mg/g. This nanocomposite could be a suitable candidate for the removal of other organic dyes.

## GRAPHICAL ABSTRACT



\* Corresponding author: Aliakbar Dehno Khalaji

✉ E-mail: [alidkhalaji@yahoo.com](mailto:alidkhalaji@yahoo.com)

☎ Tel number: +98-1732245882

© 2020 by SPC (Sami Publishing Company)



## Introduction

One of the serious global problems is water pollutants. Removal or preventing disposal of these pollutants has been one of the topics of interest in recent research [1-9]. Organic dyes are one of the most important water pollutants produced by various industrial companies [10]. These dyes can affect on the ecosystem and damage it [11]. Given the environmental problems and their imposed costs, the development of new methods with high efficiency seems necessary to remove dyes from wastewaters. In recent years, many techniques have been developed and used to remove various organic dyes from aqueous solutions such as flocculation [12], photocatalytic degradation [13], adsorption [11,14,15], nano-filtration [16], advanced oxidation [17] and biological degradation [18]. However, some of these methods suffer from complexity, high cost, and low removal efficiency [19]. Among them, adsorption has received increasing attention because the technique is cheap, simple, of low energy consumption, and effective in removing the low concentration of organic dyes [1-9] and heavy metal ions [20-22]. Cost-effectiveness, high surface area, strong binding capability to pollutants, non-toxicity, eco-friendliness and recyclability are some of the characteristics that adsorbents should have to be used for efficient removal of dyes from wastewaters [23].

Chitosan (Cs) and its modified compounds are one of the best essential materials for organic dye removal due to various active groups such as OH, NH<sub>2</sub>, C=N, NO<sub>2</sub> on the surface [1-8, 14-16, 24-28]. The free OH and NH<sub>2</sub> groups on the chitosan were easily functionalized with various compounds such as epichlorohydrin (EC) [10,20], sulfuric acid [1], quaternary ammonium salt [4], various carboxylic acids [14,16] and aldehydes [9,26,29,30]. Ke et al. [4] reported the use of quaternary ammonium salt-modified chitosan for methyl orange removal. The results indicated that at the optimum conditions, the

maximum removal rate and adsorption capacity are 98.9% and 131.9 mg/g, respectively. Gu et al. [15] developed the chitosan-lignosulfonate composite as a high adsorption efficiency of congo red. Habiba et al. [24] reported the adsorption of methyl orange on the surface of chitosan/polyvinyl alcohol/zeolite electrospun composite. Schiff-bases are among efficient materials that can be used to functionalize iron oxide surface [31]. Schiff bases could be easily produced by the reaction of the free amine group of chitosan with the carbonyl group of various compounds. The group -RC = N- obtained in these schiff bases has many potentials for analytical and environmental applications by improving the adsorption or complexation properties [32]. Sanati et al. [30] considered removing methyl green (MG) from an aqueous solution using the new modified chitosan Schiff base.

MG is a cationic dye widely used in biology and medicine as a photochromophore [33]. So far, various adsorbent has been used in the removal of MG from an aqueous solution such as MCM-41 [33], reduced graphene oxide [34], activated bentonite [35], carbon nanotube decorated with Ni nano ferrites [36], activated carbon [37] and chitosan Schiff base [30].

In this paper, chitosan was modified using epichlorohydrin, 4-hydroxybenzaldehyde (OBA), and Fe<sub>2</sub>O<sub>3</sub> nanoparticles to prepare EC-Cs-OBA-Fe<sub>2</sub>O<sub>3</sub> nanocomposite (Scheme 1). The EC-Cs-OBA-Fe<sub>2</sub>O<sub>3</sub> nanocomposite was characterized by XRD, FT-IR, TGA/DTA, DSC, EDS, BET, XRD, and FE-SEM and used as novel adsorbent for MG removal from aqueous solutions.

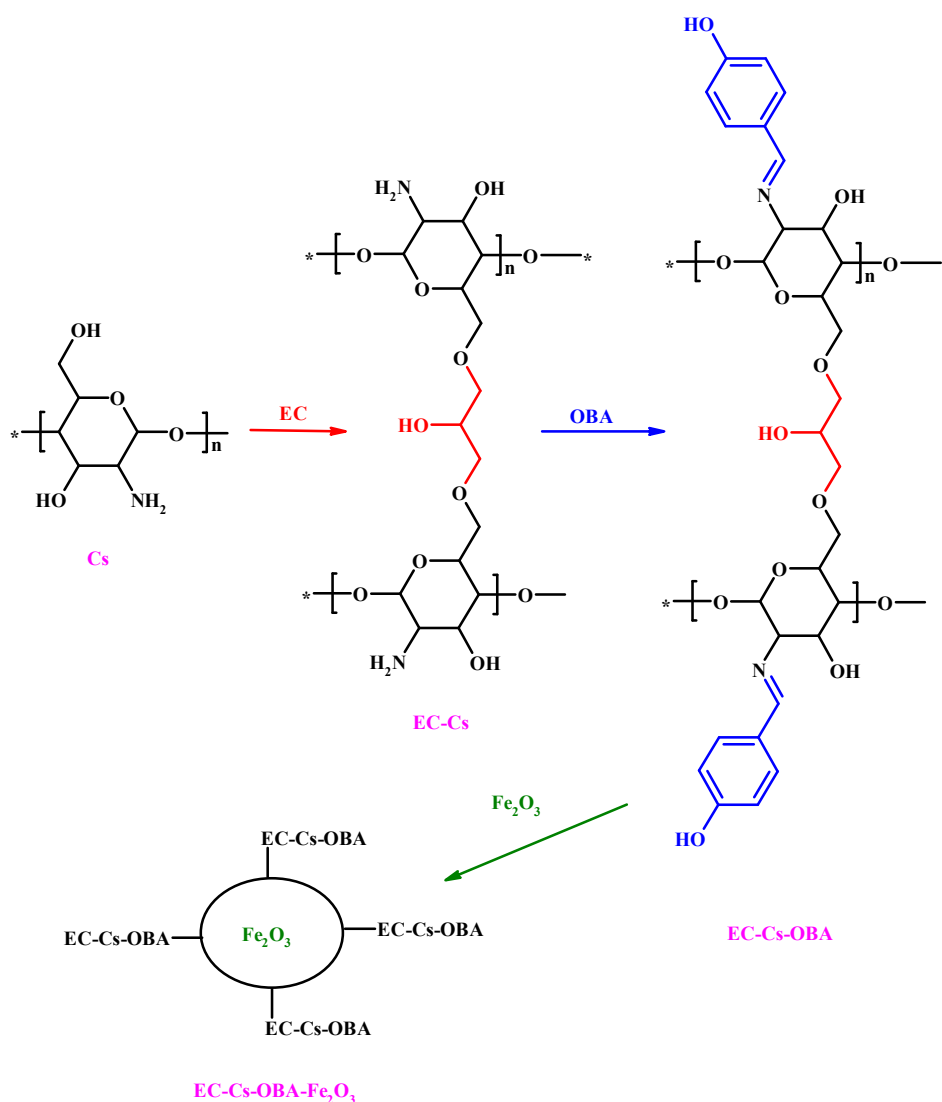
## Experimental

### Materials and methods

All reagents were of analytical grade and were purchased from Merck and Sigma-Aldrich Co. and were used as received without further purification. Fe<sub>2</sub>O<sub>3</sub> nanoparticles were prepared

according to previous literature [38]. FT-IR spectrophotometer instrument (Perkin-Elmer) was used to record FT-IR spectrum (KBr disks, 4000–400  $\text{cm}^{-1}$ ). DSC analysis was recorded by DSC analyser (Model 60A, Shimadzu, Japan). X-ray diffractometer ( $2\theta = 10\text{-}80^\circ$ , Bruker AXS-D8) was used to determine XRD pattern. SEM image and EDS data were recorded on the TESCAN Vega Model scanning electron microscope. The Perkin-Elmer TGA analyzer was used for the

thermogravimetric analysis in the air atmosphere at a flow rate of 20  $^\circ\text{C}/\text{min}$  (25–700  $^\circ\text{C}$ ). UV-Vis spectra were carried out with a UV-Visible spectrophotometer (Perkin-Elmer). The magnetic property was recorded by the vibrating sample magnetometer (VSM) with a  $5 \times 10^6$  emus sensitivity. The specific surface area of the sample was determined using the BET method (BET-Beckman colter, SA3100, USA).



**Scheme 1.** Schematic illustration of EC-Cs-OBA-Fe<sub>2</sub>O<sub>3</sub> nanocomposite preparation.

### Synthesis of EC-Cs-OBA-Fe<sub>2</sub>O<sub>3</sub> nanocomposite

2.0 g of Chitosan was suspended in 100.0 mL of ethanol-glacial acetic acid (95:5 v/v) and stirred. After 10 min, 2 mL epichlorohydrin was added and stirred for about 30 min. Then, to this mixture, ethanolic solution of 4-methoxy benzaldehyde (2 g in 10 mL) was slowly added dropwise, followed by adding 0.5 g of  $\alpha$ -Fe<sub>2</sub>O<sub>3</sub> nanoparticles; the reaction mixture was kept at 80°C, up to a brown solid precipitated. The mixture was then cooled, and the solid was filtered off, washed with cold ethanol, and dried at room temperature for several days. The product was characterized by FT-IR, XRD, TGA/DTA, DSC, EDS, BET, XRD, and FE-SEM

### Adsorption experiments

All adsorption experiments were performed in a series of 50.0 mL Erlenmeyer flasks containing the adsorbent and 25.0 mL of MG (40 mg/L) solution. The suspensions were shaken for a certain time, and then the adsorbent (EC-Cs-OBA-Fe<sub>2</sub>O<sub>3</sub>) was separated by centrifuging (4500 rpm, 15 min). The supernatant was analyzed to determine MG content using a UV-Vis spectrophotometer and corresponding calibration curve. The removal rate R (%) and adsorption capacity q<sub>t</sub> (mg/g) of MG onto the EC-Cs-OBA-Fe<sub>2</sub>O<sub>3</sub> were calculated based on the following equations [7,10,22]:

$$R = \{(C_i - C_t) \times 100\} / C_i$$

$$q_t = V \times \{(C_i - C_t) / M\}$$

Where C<sub>i</sub> (mg/L) is the initial and C<sub>t</sub> (mg/L) is the final concentration of MG, V (L) is the volume of solution, and M (g) is the mass of EC-Cs-OBA-Fe<sub>2</sub>O<sub>3</sub>.

## Results and discussion

### FT-IR spectrum

In this paper, chitosan was modified by epichlorohydrin, 4-hydroxybenzaldehyde, and Fe<sub>2</sub>O<sub>3</sub> nanoparticles. FT-IR spectrum of EC-Cs-OBA-Fe<sub>2</sub>O<sub>3</sub> in wavenumbers from 4000 to 400

cm<sup>-1</sup> is shown in Figure 1. The broad peak at 3384 cm<sup>-1</sup> is assigned to the various OH groups [3,4], while the sharp peak at 1620 is assigned to the imine group (C=N) [9,29,30,39-41] confirming the preparation of Schiff base compound. The two peaks at 558 and 471 cm<sup>-1</sup> are assigned to the Fe-O stretching vibration of Fe<sub>2</sub>O<sub>3</sub> [1,2]. The peaks at about 2860 and 2950 cm<sup>-1</sup> can be respectively assigned to the asymmetric and symmetric aliphatic hydrogens [41,42].

### TG/DTA/DSC curves

The TG/DTA curves of EC-Cs-OBA-Fe<sub>2</sub>O<sub>3</sub> are shown in Figure 2. According to Figure 2, the mass loss of EC-Cs-OBA-Fe<sub>2</sub>O<sub>3</sub> has happened in the three principal decomposition stages. In the first one,  $\approx$  20% mass loss was seen from 80 to 240 °C. The second one between 240 to 360 °C, the compound loses about 25% of its weight [9,30]. By heating the compound from 360 to 830 °C, about 17% of the mass of the compound is decomposed. Finally, at 830 °C, about 43% of the mass of the compound remains [9]. According to the DTA, the primary exothermic process was observed at 299 °C [30].

A broad weak endothermic peak was observed at 82°C, corresponding to the evaporation of the absorbed ethanol solvent, and a sharp exothermic peak was observed at 258 °C, corresponding to the decomposition of Schiff base groups [9,30] observed in the DSC curve of EC-Cs-OBA-Fe<sub>2</sub>O<sub>3</sub> (Fig. 3).

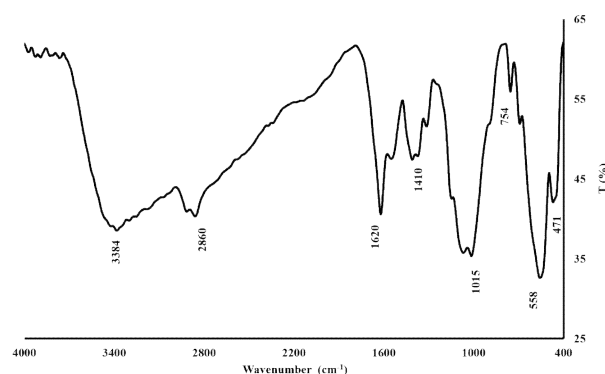
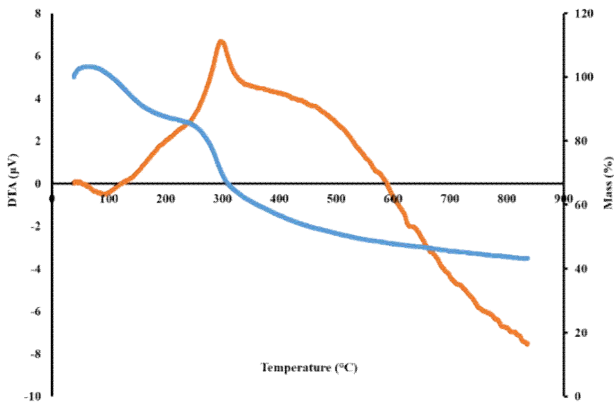


Fig 1. FT-IR spectrum of EC-Cs-OBA-Fe<sub>2</sub>O<sub>3</sub>

**XRD pattern**

In Figure 4, Chitosan exhibits a strong peak at  $2\theta = 20.01^\circ$  [3,26,34,35] and two peaks concerning  $\alpha\text{-Fe}_2\text{O}_3$  [29,36] nanoparticles were observed at  $2\theta = 33.26$  and  $35.78^\circ$  indexed to planes (104) and (101), respectively.



**Fig 2.** TG/DTA curves of EC-Cs-OBA-Fe<sub>2</sub>O<sub>3</sub>

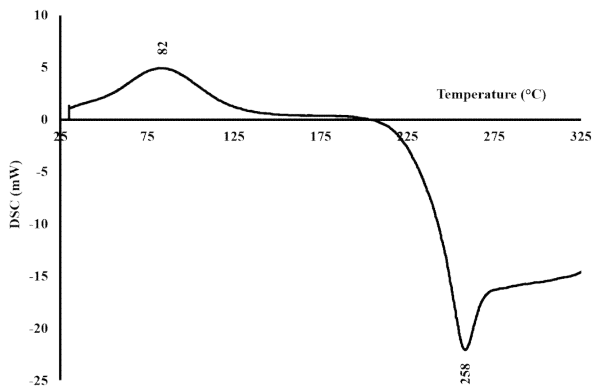


**Fig 3.** DSC curve of EC-Cs-OBA-Fe<sub>2</sub>O<sub>3</sub>

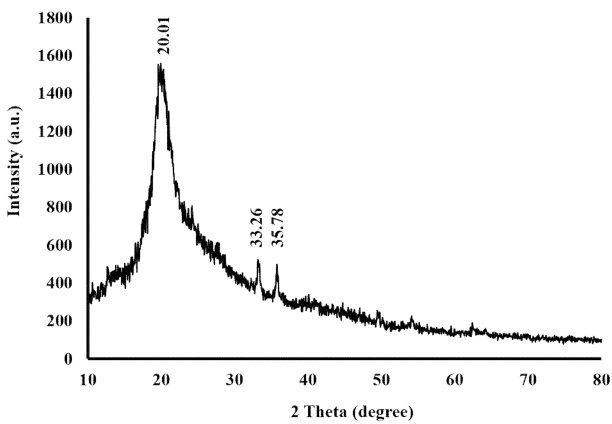


**Fig 4.** XRD pattern of EC-Cs-OBA-Fe<sub>2</sub>O<sub>3</sub>

**SEM images and EDS data**

The study of morphology and particle size of EC-Cs-OBA-Fe<sub>2</sub>O<sub>3</sub> nanocomposite and SEM images were obtained as shown in Figure 5. As seen in Figure 5, the quasi-spherical Fe<sub>2</sub>O<sub>3</sub> nanoparticles were loaded on the surface of chitosan. However, the Fe<sub>2</sub>O<sub>3</sub> nanoparticles formed aggregate. The surface of EC-Cs-OBA is almost smooth. The average crystalline size of Fe<sub>2</sub>O<sub>3</sub> nanoparticles is about 45 nm.

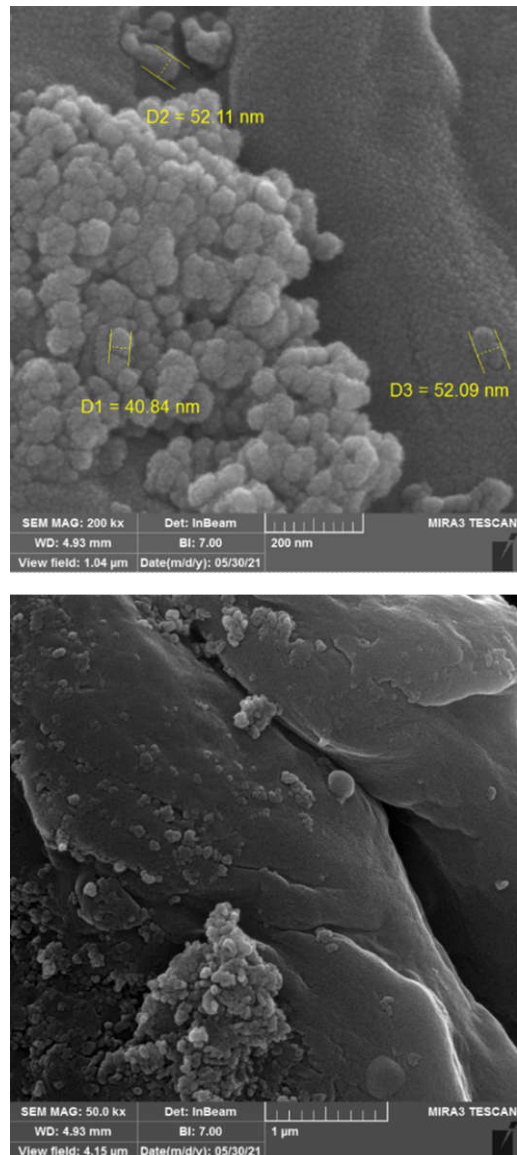


**Fig 5.** SEM images of EC-Cs-OBA-Fe<sub>2</sub>O<sub>3</sub> with two different scales

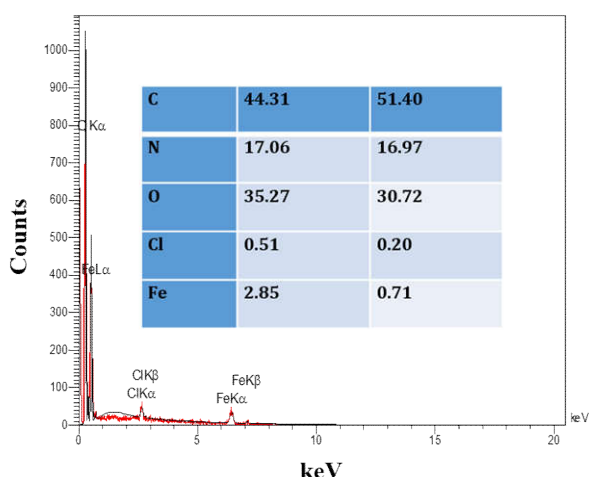


**Fig 6.** SEM-EDS data of EC-Cs-OBA-Fe<sub>2</sub>O<sub>3</sub>

The SEM-EDS data of EC-Cs-OBA-Fe<sub>2</sub>O<sub>3</sub> is shown in Figure 6. The main elements in the EC-Cs-OBA-Fe<sub>2</sub>O<sub>3</sub> nanocomposite are C (44.31%) and O (35.27%), respectively. However, the Fe mass percentage is 2.85%.

#### VSM analysis

Figure 7 shows the magnetic properties of EC-Cs-OBA-Fe<sub>2</sub>O<sub>3</sub> nanocomposite. The saturation magnetization value is 0.03 emu/g. The low magnetic saturation predicts the low concentration of Fe<sub>2</sub>O<sub>3</sub> in the EC-Cs-OBA-Fe<sub>2</sub>O<sub>3</sub>. SEM-EDS data confirm this matter.

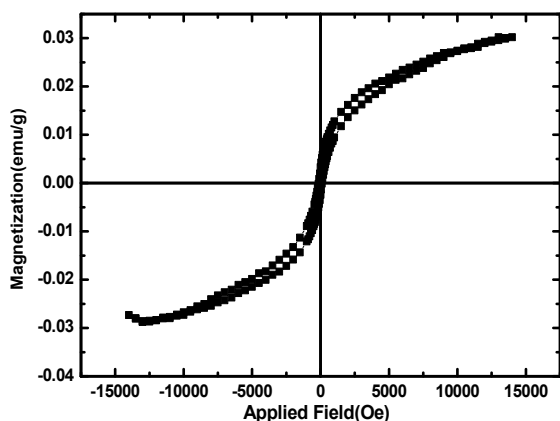


**Fig 7.** VSM of EC-Cs-OBA-Fe<sub>2</sub>O<sub>3</sub>

#### MG removal studies

The effect pH (2-10), adsorbent weigh (0.005, 0.01, and 0.02 g) and contact times (0-30 min) were evaluated on the MG adsorption.

#### Solutions pH

At first, we considered the initial pH solution as an essential factor on the MG removal percentage by varying it from 2 to 10 under constant other parameters such as contact time (30 min), initial MG concentration (40 mg/L), adsorbent dosage (0.01 g) and temperature (25 °C) as shown in Figure 8. At low pHs, there is a competition between hydrogen ions and dye molecules for interaction with the adsorbent. Due to the smaller size of the hydrogen ions, these ions interact much more easily with the adsorbent and inactivate the adsorbent sites. Therefore, methyl green cannot be effectively absorbed [30]. As seen in Figure 8, the best pH solution for maximum removal percentage of MG is 8 due to the increases of electrostatic interaction between the various groups of MG and active sites EC-Cs-OBA-Fe<sub>2</sub>O<sub>3</sub> nanocomposite. Similar results have been reported by Sanati et al. [30] and Rida et al. [37]. So, we selected this pH for studying other parameters on the MG removal.

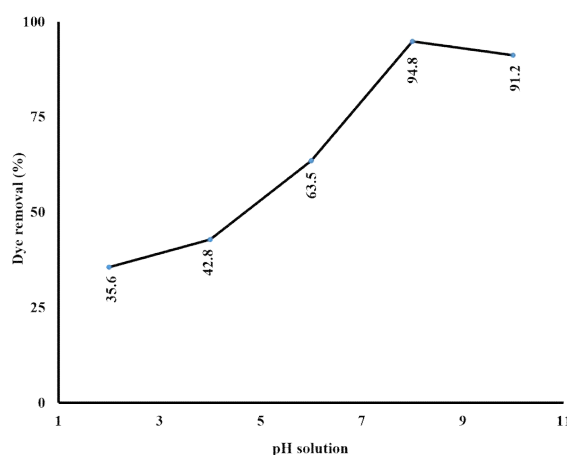


**Fig 8.** Effect of initial pH on MG removal percentage.

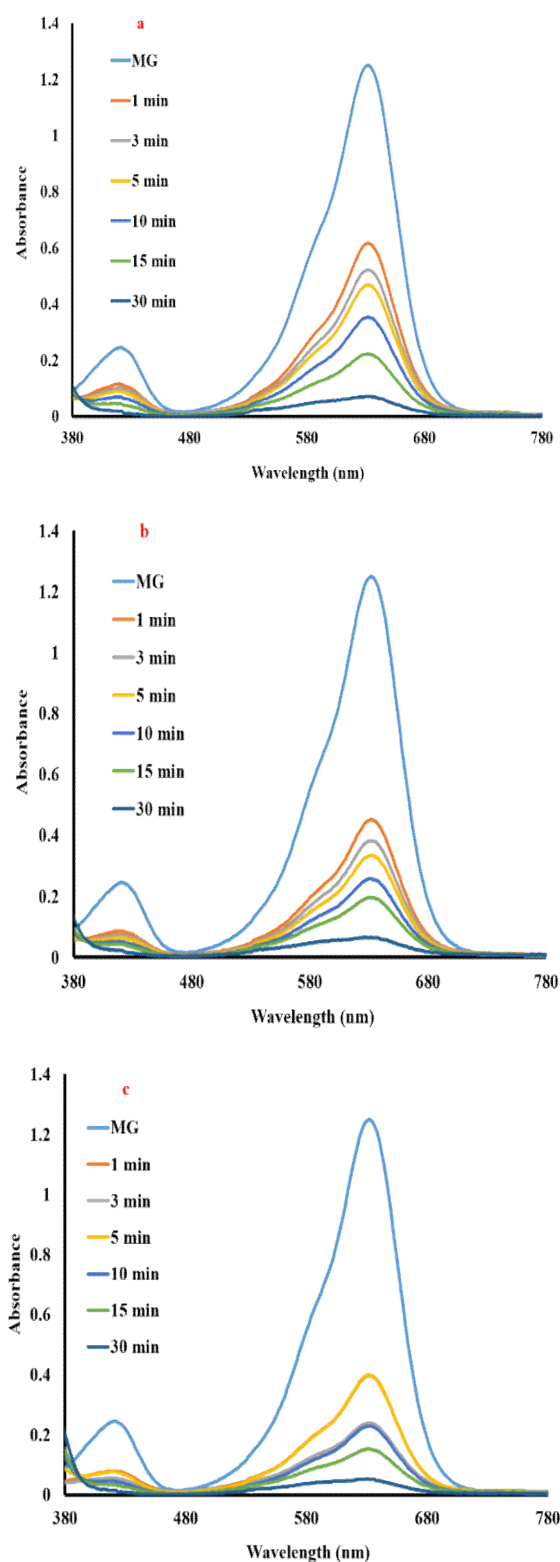


**Fig 9.** UV -Vis spectra of MG, different contact times and sorbent dosage a) 0.005, b) 0.01, and c) 0.02 g

#### *Effect of contact times and adsorbent dosages*

UV-Vis spectra of MG in different contact times and adsorbent dosages are represented in Figure 9. MG has a sharp absorption at 632 nm (due to  $n \rightarrow \pi^*$  transition). The decrease of this absorbance with increases of adsorbent dosages and contact times confirmed the removal of MG.

Table 1 shows a comparison of the adsorbent used in this study with other methods in terms of contact time, adsorbent capacity and removal efficiency of methyl green. These results show that the EC-Cs-OBA- $\text{Fe}_2\text{O}_3$  nanocomposites are very efficient for MG removal. After about 30 min the adsorption peak at 632 nm disappeared, indicating the good removal of MG. Also, there is no significant change in this peak during the adsorption study [25].

The removal percentage of MG was increased by contact time and adsorbent dosages, and finally, equilibrium was obtained after 30 min.

#### **Conclusion**

In summary, new epichlorohydrin crosslinked Schiff base chitosan/ $\text{Fe}_2\text{O}_3$  (EC-Cs-OBA- $\text{Fe}_2\text{O}_3$ ) nanocomposite was prepared by simple and low-cost condensation method, characterized, and used as adsorbent in the removal of MG. The adsorption results showed that the initial pH, contact time, and adsorbent dosage greatly affected the MG removal. Compared with other methods, the proposed method has a short contact time, high adsorption capacity and high removal efficiency.

#### **Acknowledgments**

The present study was supported by Golestan University. We thank Golestan University and Islamic Azad University for their scientific help.

**Table 1.** Comparison of the various adsorbent

Adsorbent	Removal (%)	q <sub>t</sub> (mg/g)	t (min)	Ref
Bamboo	79.4	15.5	140	46
MCM-41	49.57	20.97	1500	33
Activated Bentonite	98	353.33	180	35
NiFe <sub>2</sub> O <sub>4</sub> -CNTs	56.19	181.2	120	36
Activated Carbon	78	67.93	75	37
Sejnane Clay	99.8	20	20	47
Mesoporous Silica SBA-S4	98.4	39.4	8	19
EC-Cs-OBA-Fe <sub>2</sub> O <sub>3</sub>	94.8	47.4	30	This study

## References

- [1] Rahmi, Ismaturrehmi, I. Mustafa, Methylene blue removal from water using H<sub>2</sub>SO<sub>4</sub> crosslinked magnetic chitosan nanocomposite beads. *Microchem. J.* 144 (2019) 397-402.
- [2] D. Yang, L. Qiu, Y. Yang, Efficient adsorption of methyl orange using a modified chitosan magnetic composite adsorbent, *J. Chem. Eng. Data* 61 (2016) 3933-3940.
- [3] F.C. Tsai, N. Ma, T.C. Chiang, L.C. Tsai, J.J. Shi, Y. Xia, T. Jiang, S.K. Su, F.S. Chuang, Adsorptive removal of methyl orange from aqueous solution with crosslinking chitosan microspheres, *J. Water Process Eng.* 1 (2014) 2-7.
- [4] P. Ke, D. Zeng, K. Xu, J. Cui, G. Wang, Preparation of quaternary ammonium salt-modified chitosan microspheres and their application in dyeing wastewater treatment, *ACS Omega* 5 (2020) 24700-24707.
- [5] Y. Haldorai, J.J. Shim, An efficient removal of methyl orange dye from aqueous solution by adsorption onto chitosan/MgO composite: A novel reusable adsorbent, *App. Surf. Sci.* 292 (2014) 447-453.
- [6] L. Obeid, A. Bee, D. Talbot, S. Ben Jaafar, V. Dupuis, S. Abramson, V. Cabuil, M. Welschbillig, Chitosan/maghemite composite: A megisorbent for the adsorption of methyl orange, *J. Coll. Interface Sci.* 410 (2013) 52-58.
- [7] G. Yuvaraja, D.Y. Chen, J.L. Pathak, J. Long, M.V. Subbaiah, J.C. Wen, C.L. Pan, Preparation of novel aminated chitosan schiff's base derivative for the removal of methyl orange dye from aqueous environment and its biological applications, *Int. J. Biol. Macromol.* 146 (2020) 1100-1110.
- [8] L. Zhai, Z. Bai, Y. Zhu, B. Wang, W. Luo, Fabrication of chitosan microspheres for efficient adsorption of methyl orange, *Chin. J. Chem. Eng.* 26 (2018) 657-666.
- [9] A. Foroughnia, A.D. Khalaji, E. Kolvari, N. Koukabi, Synthesis of new chitosan Schiff base and its Fe<sub>2</sub>O<sub>3</sub> nanocomposite: Evaluation of methyl orange removal and antibacterial activity, *Int. J. Biol. Macromol.* 177 (2021) 83-91.
- [10] P.M.O. Silva, J.E. Francisco, J.C.M. Cajé, R.J. Cassella, W.F. Pacheco, A bath and fixed bed column study for fluorescein removal using chitosan modified by epichlorohydrin, *J. Environ. Sci. Health, A.* 53 (2018) 55-64.
- [11] W.A. Khanday, F. Marrakchi, M. Asif, B.H. Hameed, Mesoporous zeolite-activated carbon composite from oil palm ash as an effective adsorbent for methylene blue. *J. Taiwan Inst. Chem. Eng.* 70 (2017) 32-41.
- [12] V. Golob, A. Vinder, M. Simonic, Efficiency of the coagulation/flocculation method for the treatment of dye bath effluents, *Dye Pig.* 67 (2005) 93-97.
- [13] M. Tabatabaee, S.A. Mirrahimi, Photodegradation of dye pollutant on Ag/ZnO

- nanocatalyst under UV-irradiation. *Orient. J. Chem.* 27 (2011) 65.
- [14] M.H. Mahaninia, Sorption study of water vapor and a dye on chitosan-based framework materials, *ACS Omega* 5 (2020) 21836-21843.
- [15] F. Gu, J. Geng, M. Li, J. Chang, Y. Dui, Synthesis of chitosan-lignosulfonate composite as an adsorbent for dyes and metal ions removal from wastewater, *ACS Omega* 4 (2019) 21421-21430.
- [16] J. Wang, X. Yang, D. Zheng, A. Yao, D. Hua, V. Srinivasapriyan, G. Zhan, Fabrication of bioinspired gallic acid-grafted chitosan/polysulfone composite membranes for dye removal via nanofiltration, *ACS Omega* 5 (2020) 13077-13086.
- [17] V.K. Saharan, M.P. Badve, A.B. Pandit, Degradation of reactive red 120 dye using hydrodynamic cavitation, *Chem. Eng. J.* 178 (2011) 100-107.
- [18] A.N. Kulkarni, A.A. Kadam, M.S. Kachole, S.P. Govindwar, Lichen permelia perlata: a novel system for biodegradation and detoxification of disperse dye solvent red 24, *J. Hazard. Mater.* 276 (2014) 461-468.
- [19] L. Arjomandi-Behzad, M.K. Rofouei, A. Badiei, J. B. Ghasemi. "Simultaneous removal of crystal violet and methyl green in water samples by functionalised SBA-15." *Int. J. Environ. Anal. Chem.* (2020) 1-17.
- [20] M. Sahin, N. Kocak, G. Arslan, H.I. Ucan, Synthesis of crosslinked chitosan with epichlorohydrin possessing two novel polymeric ligands and its use in metal removal, *J. Inorg. Organomet. Polym.* 21 (2011) 69-80.
- [21] M. Li, Z. Zhang, R. Li, J.J. Wang, A. Ali, Removal of Pb(II) and Cd(II) ions from aqueous solution by thiosemicarbazide modified chitosan, *Int. J. Biol. Macromol.* 86 (2016) 876-884.
- [22] R. Ahmad, A. Mirza, Facile one pot green synthesis of chitosan-iron oxide (CS-Fe<sub>2</sub>O<sub>3</sub>) nanocomposite: Removal of Pb(II) and Cd(II) from synthetic and industrial wastewater, *J. Clean. Prod.* 186 (2018) 342-352.
- [23] M. Sajid, M.K. Nazal, N. Baig, A.M. Osman. "Removal of heavy metals and organic pollutants from water using dendritic polymers based adsorbents: a critical review." *Sep. Purif. Technol.* 191 (2018) 400-423.
- [24] U. Habiba, T.A. Siddique, S.J.L. Lee, T.C. Joo, B.C. Ang, A.M. Afifi. Adsorption study of methyl orange by chitosan/polyvinyl alcohol/zeolite electrospun composite nanofibers membrane, *Carbohydr. Polym.* 191 (2018) 79-85.
- [25] S. Kumar, B. Krishnakumar, A.J.F.N. Sobral, J. Koh, Bio-based (chitosan/PVA/ZnO) nanocomposites film: Thermally stable and photoluminescence material for removal of organic dye, *Carbohydr. Polym.* 205 (2019) 559-564.
- [26] N. Parshi, D. Pan, V. Dhavle, B. Jana, S. Maity, J. Ganguly, Fabrication of lightweight and reusable salicylaldehyde functionalized chitosan as adsorbent for dye removal and its mechanism, *Int. J. Biol. Macromol.* 141 (2019) 626-635.
- [27] S.A. Hosseini, S. Daneshvar e Asl, M. Vossoughi, A. Simchi, M. Sadrzadeh, Green electrospun membranes based on chitosan/amino functionalized nanoclay composite fibers for cationic dye removal: Synthesis and kinetic studies, *ACS Omega* 6 (2021) 10816-10827.
- [28] S. Cinar, U.H. Kaynar, T. Aydemir, S.C. Kaynar, M. Ayvacikli, An efficient removal of RB5 from aqueous solution by adsorption onto nano-ZnO/chitosan composite beads, *Int. J. Biol. Macromol.* 96 (2017) 459-465.
- [29] M.S. Hussain, S.G. Musharraf, M.I. Bhangar, M.I. Malik, Salicylaldehyde derivative of nano-chitosan as an efficient adsorbent for lead(II), copper(II), and cadmium(II) ions, *Int. J. Biol. Macromol.* 147 (2020) 643-652.
- [30] M. Sanati, A.D. Khalaji, A. Mokhtari, M. Keyvanfard, Fast removal of methyl green

- from aqueous solution by adsorption onto new modified chitosan Schiff base, *Prog. Chem. Biochem. Res.* 4(3) (2021) 319-330.
- [31] M. Setoodehkhah, S. Momeni. "Water Soluble Schiff Base Functionalized Fe<sub>3</sub>O<sub>4</sub> Magnetic Nano-Particles as a Novel Adsorbent for the Removal of Pb (II) and Cu (II) Metal Ions from Aqueous Solutions." *J. Inorg. Organomet. Polym. Mater.* 28 (2018) 1098-1106.
- [32] E.M. El-Sayed, T. M. Tamer, A. M. Omer, M. S. Mohy Eldin. "Development of novel chitosan schiff base derivatives for cationic dye removal: methyl orange model." *Desalin. Water Treat.* 57 (2016) 22632-22645.
- [33] S.M. Alardhi, T.M. Albayati, J.M. Alrubaye, Adsorption of the methyl green dye pollutant from aqueous solution using mesoporous materials MCM-41 in a fixed-bed column, *Heliyon* 6 (2020) e03253.
- [34] P. Sharma, b.K. Saikia, M.R. Das, Removal of methyl green dye molecule from aqueous system using reduced graphene oxide as an efficient adsorbent: kinetics, isotherm and thermodynamic parameters, *Coll. Surf. A.* 457 (2014) 125-133.
- [35] A. Maghni, M. Ghelamallah, A. Benghalem, Sorptive removal of methyl green from aqueous solutions using activated bentonite, *Acta Phys. Pol. A.* 132 (2017) 448-450.
- [36] M. Bahgat, A.A. Farghali, W. El Rouby, M. Khedr, M.Y. Mohassab-Ahmed, Adsorption of methyl green dye onto multi-walled carbon nanotubes decorated with Ni nanoferrite, *App. Nanosci.* 3 (2013) 251-261.
- [37] K. Rida, K. Chaibedra, K. Cheraitia, Adsorption of cationic dye methyl green from aqueous solution onto activated carbon prepared from *Brachychiton Populneus* fruit shell, *Ind. J. Chem. Technol.* 27 (2020) 51-59.
- [38] A.D. Khalaji, S.M. Mousavi, M. Jarosova, P. Machek, The effect of calcination on the morphology, size and the crystalline phase of the as-synthesized products by direct calcination of FeSO<sub>4</sub> at the presence of benzoic acid, *J. Surf. Invest. X-ray, Synch. Neut. Tech.* 14 (2020) 1191-1194.
- [39] K.R. Ansari, D.S. Chauhan, M.A. Quraishi, M.A.J. Mazumder, A. Singh, Chitosan Schiff base: an environmentally benign biological macromolecule as a new corrosion inhibitor for oil & gas industries, *Int. J. Biol. Macromol.* 144 (2020) 305-315.
- [40] S. Shahraki, H.S. Delarami, F. Khosravi, Synthesis and characterization of an adsorptive Schiff base – chitosan nanocomposite for removal of Pb(II) ion from aqueous media, *Int. J. Biol. Macromol.* 139 (2019) 577-586.
- [41] M.M. Iftime, S. Morarium L. Marin, Salicyl-imine-chitosan hydrogels: supramolecular architeturings as a crosslinking method toward multifunctional hydrogels, *Carbohydr. Polym.* 165 (2017) 39-50.
- [42] W.S. Wan Ngah, M.A.K.M. Hanafiah, S.S. Yong, Adsorption of humic acid from aqueous solutions on crosslinked chitosan-epichlorohydrin beads: Kinetics and isotherm studies, *Coll. Surf. B.* 65 (2008) 18-24.
- [43] Z. Weijiang, Z. Yace, G. Yuvaraja, X. Jiao, Adsorption of Pb(II) from aqueous environment using eco-friendly chitosan Schiff's base@Fe<sub>3</sub>O<sub>4</sub> (CSB@Fe<sub>3</sub>O<sub>4</sub>) as an adsorbent: kinetic, isotherm and thermodynamic studies, *Int. J. Biol. Macromol.* 105 (2017) 422-430.
- [44] Y. Yan, G. Yuvaraja, C. Liu, L. Kong, K. Guo, G.M. Reddy, G.V. Zyryanov, Removl of Pb(II) ions from aqueous media using epichlorohydrin crosslinked chitosan Schiff's base@Fe<sub>3</sub>O<sub>4</sub> (ECCSB@Fe<sub>3</sub>O<sub>4</sub>), *Int. J. Biol. Macromol.* 117 (2018) 1305-1313.
- [45] R. Ahmad, A. Mirza, Facile one pot green synthesis of chitosan-iron oxide (CD-Fe<sub>2</sub>O<sub>3</sub>) nanocomposite: Removal of Pb(II) and Cd(II) from synthetic and industrial wastewater, *J. Clean Produc.* 186 (2018) 342-352.
- [46] A.A. Atshan, "Adsorption of methyl green dye onto bamboo in batch and continuous

system." *Iraqi J. Chem. Pet. Eng.* 15 (2014) 65-72.

[47] Y. Satlaoui, M. Trifi, D.F. Romdhane, A. Charef, R. Azouzi. "Removal properties,

mechanisms, and performance of methyl green from aqueous solution using raw and purified Sejnane clay type." *J. Chem.* 2019 (2019) 4121864.

#### HOW TO CITE THIS ARTICLE

Arefeh Khalili, Aliakbar Dehno Khalaji, Ali Mokhtari, Mohsen Keyvanfard, Synthesis, Characterization, and Methyl Green Removal of Epichlorohydrin Crosslinked Schiff Base Chitosan/Fe<sub>2</sub>O<sub>3</sub> Nanocomposite, *Prog. Chem. Biochem. Res.* 4(4) (2021) 392-402.

**DOI:** 10.22034/pcbr.2021.290770.1192

**URL:** [http://www.pcbiochemres.com/article\\_141624.html](http://www.pcbiochemres.com/article_141624.html)

